The Plant Cell, Vol. 10, 937–946, June 1998, www.plantcell.org © 1998 American Society of Plant Physiologists

Initiation and Maintenance of Virus-Induced Gene Silencing

M. Teresa Ruiz,[1] Olivier Voinnet,[1] and David C. Baulcombe[2]

Sainsbury Laboratory, John Innes Centre, Colney, Norwich NR4 7UH, United Kingdom

The phytoene desaturase (PDS) gene of *Nicotiana benthamiana* was silenced in plants infected with potato virus X (PVX) vectors carrying PDS inserts, and a green fluorescent protein (GFP) transgene was silenced in plants infected with PVX–GFP. This virus-induced gene silencing (VIGS) is post-transcriptional and cytoplasmic because it is targeted against exons rather than introns of PDS RNA and against viral RNAs. Although PDS and GFP RNAs are most likely targeted through the same mechanism, the VIGS phenotypes differed in two respects. PDS mRNA was targeted by VIGS in all green tissue of the PVX–PDS—infected plant, whereas PVX–PDS was not affected. In contrast, VIGS of the GFP was targeted against PVX–GFP. Initially, VIGS of the GFP was initiated in all green tissues, as occurred with PDS VIGS. However, after 30 days of infection, the GFP VIGS was no longer initiated in newly emerging leaves, although it was maintained in tissue in which it had already been initiated. Based on these analyses, we propose a model for VIGS in which the initiation of VIGS is dependent on the virus and maintenance of it is virus independent.

INTRODUCTION

Virus-induced gene silencing (VIGS) in plants takes place if there is sequence similarity between the virus and either a transgene or an endogenous nuclear gene (Lindbo et al., 1993; Kumagai et al., 1995). From the examples involving viral transgenes, it is known that the mechanism is post-transcriptional and can be targeted, in a sequence-specific manner, against the transgene mRNA as well as the RNA genome of the virus (Lindbo et al., 1993; Smith et al., 1994; Goodwin et al., 1996; Guo and Garcia, 1997). Because these examples involve cytoplasmic RNA viruses, it was inferred that the mechanism of VIGS involves destabilization of the target mRNAs in the cytoplasm (Smith et al., 1994).

Post-transcriptional gene silencing also takes place in transgenic plants without virus infection (Baulcombe, 1996b; Depicker and Van Montagu, 1997). However, like VIGS, these examples of transgene-induced gene silencing can be targeted against viral RNAs (English et al., 1996; Sijen et al., 1996), and it is likely that similar mechanisms are involved (Tanzer et al., 1997). Many of the reported examples of pathogen-derived resistance are probably manifestations of transgene-induced silencing targeted against viral RNA (Baulcombe, 1996b).

These reports that viruses can both initiate and be targets of gene silencing have prompted speculation that the mechanism is part of a defense system in plants against viruses (Baulcombe, 1996a; Pruss et al., 1997). According to this idea, gene silencing would be activated naturally in virus-infected plants and artificially in transgenic plants when the transgene or its RNA is perceived as part of a virus. Consistent with this proposal are examples of virus-induced virus resistance in nontransgenic plants (Covey et al., 1997; Ratcliff et al., 1997) that resemble gene silencing because the mechanism is targeted against RNA in a sequence-specific manner.

Here, we provide an analysis of VIGS that was designed to shed light on the mechanism of VIGS and the relationship of VIGS, post-transcriptional gene silencing, and antiviral defense. We compare VIGS targeted against a green fluorescent protein (GFP) transgene (Chalfie et al., 1994; Baulcombe et al., 1995; Haseloff et al., 1997) and an endogenous phytoene desaturase (PDS) gene. Based on the different features of VIGS in these systems, we produce a model in which the mechanism of VIGS involves separate initiation and maintenance stages. Our findings show that VIGS and transgene-mediated gene silencing are similar and reinforce the predicted role of gene silencing in natural virus defense.

RESULTS

Gene Silencing by Potato Virus X Vectors with PDS Inserts

To investigate VIGS, we initially targeted the PDS gene of *Nicotiana benthamiana* by using potato virus X (PVX) vectors carrying inserts of PDS cDNA. VIGS of PDS causes suppression of carotenoid biosynthesis so that the affected plants would be susceptible to photobleaching (Demmig-Adams and Adams, 1992). Figure 1A shows the construction of the PVX vectors carrying a 415-nucleotide fragment from the central region

[1] Both authors contributed equally to this work.

[2] To whom correspondence should be addressed. E-mail baulcombe@bbsrc.ac.uk; fax 44-1603-250024.

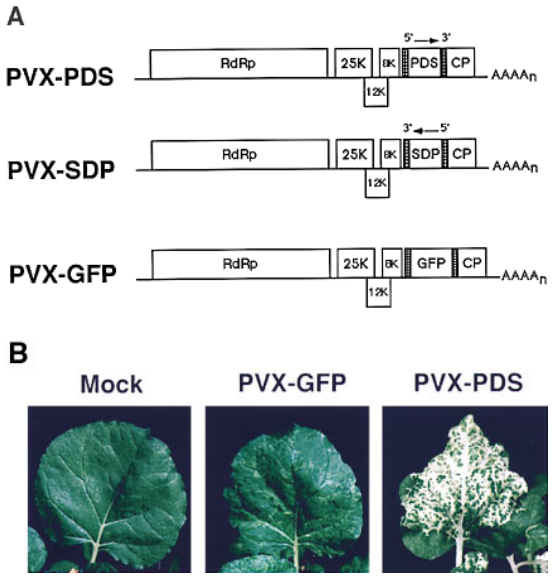

Figure 1. VIGS of PDS.

(A) Genomic organization of PVX vectors used in VIGS analysis of PDS. The PVX open reading frames are shown as RdRp (RNA-dependent RNA polymerase), 25K (25K protein), 12K (12K protein), 8K (8K protein), and CP (coat protein), and the inserts were a fragment from the PDS open reading frame in the sense (PDS) or antisense (SDP) orientation. The GFP construct (PVX–GFP) was used as a control. The vector constructs were assembled as cDNA and transcribed into RNA for inoculation of plants. $AAAA_n$ represents the 3′-terminal polyA of the PVX genome.
(B) Systemic leaves of plants that were either mock inoculated or inoculated with PVX–GFP or PVX–PDS, as indicated. The leaves were photographed at 24 DPI.

of the PDS open reading frame cloned into PVX in the sense (PVX–PDS) or antisense (PVX–SDP) orientation.

N. benthamiana plants inoculated with transcripts of these constructs generated in vitro developed bleaching in the systemic leaves 10 to 15 days postinoculation (DPI). At first, the bleached regions were confined to the leaf veins. Later, as shown in Figure 1B (PVX–PDS), the photobleaching symptoms extended to most of the foliar tissue, although there was always a mosaic of green and white tissue. Stems, axillary shoots, sepals, and seed capsules were all affected, and tissues emerging as late as 2 months postinoculation continued to show bleaching. The PVX–PDS and PVX–SDP constructs both caused VIGS to the same extent and over the same time course. In contrast, the plants inoculated with a PVX vector carrying an insert unrelated to PDS, such as GFP (Figure 1B; PVX–GFP), showed only a light green mosaic. From these data, we conclude that PVX vectors can cause VIGS, as reported previously for tobacco mosaic virus (TMV) vectors with PDS inserts (Kumagai et al., 1995).

The ability of different parts of the PDS gene to cause VIGS was investigated using the PVX vectors shown in Figure 2. The inserts in these vectors are from PDS genomic DNA and cDNA and include a 212-nucleotide fragment from within the fragment carried in PVX–PDS (PVX–PDS^{def} and PVX–SDP^{def}, depending on the orientation); a 223-nucleotide fragment from an intron that is spanned by PVX–PDS^{def} (PVX–INT and PVX–TNI); a 377-nucleotide region from an exon beginning at the PDS initiation codon (PVX–5′PDS and PVX–5′SDP); and a 167-nucleotide region that includes an intron in the 5′ untranslated region upstream of the initiation codon (PVX–5′UTR and PVX–5′RTU).

Of these vectors, only those with introns (PVX–INT, PVX–TNI, PVX–5′UTR, and PVX–5′RTU) failed to cause VIGS (Figure 2). The lack of VIGS with the intron vectors suggests that the mechanism is initiated in the cytoplasm and/or targeted against cytoplasmic RNA and indicates that VIGS of PDS is post-transcriptional. The finding that the 5′PDS as well as the PDS constructs caused gene silencing shows that the potential to cause VIGS is not restricted to a single region in the PDS mRNA sequence.

Effect of VIGS on PDS mRNA and Virus Accumulation

To monitor the level of the low-abundance mRNA for PDS, we subjected samples taken at 24 DPI to reverse transcription followed by polymerase chain reaction (RT-PCR), as performed in a previous analysis of PDS mRNA in tomato

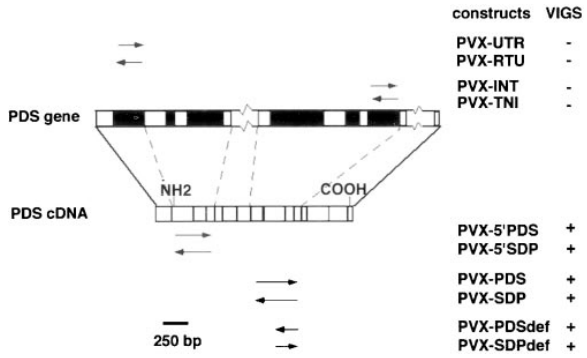

Figure 2. VIGS by Different Regions of PDS Genomic and mRNA Sequences.

The *N. benthamiana* PDS genomic sequence includes exons (open boxes) and introns (closed boxes) that were identified by alignment with the tomato genomic sequence (Mann et al., 1994). Parts of the *N. benthamiana* genomic sequence have not been determined (zigzag lines). The initiation and termination codons of the PDS cDNA are indicated as NH_2 and COOH. The PVX constructs listed were assembled by insertion of the indicated regions of PDS genomic or cDNA into the PVX cDNA vector (see Methods). Arrows indicate the orientation of the insert. The constructs were transcribed into RNA for inoculation. The ability of the constructs to mediate VIGS of PDS at 24 DPI is indicated as (+) or (−) in the right-hand column.

(Giuliano et al., 1993). The results shown in Figure 3A reveal that PDS mRNA was 85 to 95% less abundant in the systemic tissue of PVX–PDS—infected tissue than in mock-inoculated tissue or in tissue infected with PVX–GFP (data not shown). The reduction in PDS mRNA was similar in both green and white areas of the PVX–PDS—infected plants (Figure 3A), indicating that some degree of photoprotection is obtained even when PDS levels are suppressed. Clearly, the photobleaching symptom does not reflect the full extent of the PVX–PDS—induced gene silencing.

Figure 3B illustrates the results of gel blot analysis using either PVX or PDS as probes. This analysis was performed to determine whether the PVX–PDS or PVX–SDP RNAs could be a target of VIGS and shows that at 24 DPI, the PVX vectors with PDS or SDP inserts accumulated at high levels in both the green and white tissues. Wild-type PVX, which did not induce PDS gene silencing, also accumulated at similarly high levels (Figure 3B). The high levels of PVX–PDS were maintained in five independent experiments in tissue that was sampled up to 45 DPI. We conclude from these experiments that the PVX–PDS and PVX–SDP RNAs were not targets of VIGS. This conclusion was reinforced by other analyses showing that PVX–PDS and PVX–SDP accumulated unaltered in the green and white tissue of the bleached plants (data not shown). For example, in plants inoculated with sap extracts from both white and green silenced tissue, the silencing phenotype developed as quickly and to the same extent as in the transcript-inoculated plants. Moreover, RT-PCR of PVX RNA in samples from both green and white tissue revealed only PVX–PDS or PVX–SDP. Similar results were obtained with other constructs (Figure 2) that were able to induce VIGS of PDS (data not shown).

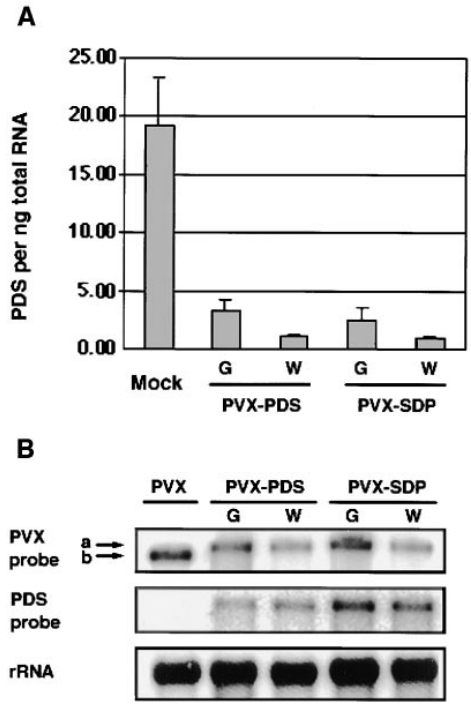

Figure 3. PDS RNA Levels.

(A) PDS mRNA levels in mock-inoculated or PVX–PDS— and PVX–SDP—inoculated plants were determined by RT-PCR, using ubiquitin mRNA as internal standard and expressed as photostimulated luminescence units per nanogram of total RNA (see Methods). RNA samples were harvested at 24 DPI from green (G) or white (W) tissue of the infected plants. Error bars represent SE.

(B) PVX, PVX–PDS, and PVX–SDP in systemically infected leaves. The RNA samples were taken at 24 DPI when the PVX–PDS— and PVX–SDP—infected plants exhibited strong photobleaching due to VIGS. Equal amounts of each RNA sample (1.5 mg) were fractionated by agarose gel electrophoresis. The filter was first hybridized with a ^{32}P-labeled cDNA PDS probe (positions 1300 to 1712; see Methods) to detect the presence of the insert and then with a ^{32}P-labeled RNA probe for PVX to detect the viral RNAs. The major genomic RNA is shown. The filter was finally probed with a ^{32}P-labeled ribosomal cDNA to show equal loading. The migration of the PVX RNA (a) in extracts of plants infected with PVX–PDS and PVX–SDP was slower than was the migration of the RNA of wild-type PVX (b), thereby illustrating that the accumulated RNA had not developed the ability to overcome VIGS due to loss of the PDS-derived insert.

Virus-Induced Silencing of a 35S-GFP Transgene

To further investigate the mechanism of VIGS, we targeted a GFP transgene (Haseloff et al., 1997) so that the silencing could be monitored noninvasively by UV illumination of the infected plants. Four independent lines of *N. benthamiana* carrying a GFP transgene under the control of the cauliflower mosaic virus 35S promoter were generated by agrotransformation. Figure 4A is a diagram of the T-DNA constructs used to generate these transgenic lines. Each of the lines carries transgenes at a single locus, and the experiments described here were performed with progeny in which the transgene locus was in the homozygous condition. Figure 4B illustrates the green fluorescence of leaves and stems of these transgenic plants. The nontransgenic tissue appeared red because of chlorophyll fluorescence (Figure 4B). To investigate VIGS, the GFP lines were inoculated with PVX–GFP encoding the intact GFP or with PVX–GF in which the 470-nucleotide insert lacked the 3′ end of the GFP coding sequence (Figure 4A). PVX–GF(P) refers to both PVX–GFP and PVX–GF. To avoid confusion, we refer to intGFP from the integrated transgene and vGFP from the PVX–GF(P). Although the data presented are all from one line (line GFP8), similar data were obtained with all four lines.

The response to PVX–GFP in these plants followed three phases. Initially, the transgenic plants exhibited vGFP fluorescence superimposed on the fluorescence from the intGFP. In plants inoculated with PVX–GF, there was no vGFP fluorescence. The second phase of the response started at 8 DPI in localized regions of the inoculated leaf and at 10 to 15 DPI in parts of the systemic tissue and was characterized by

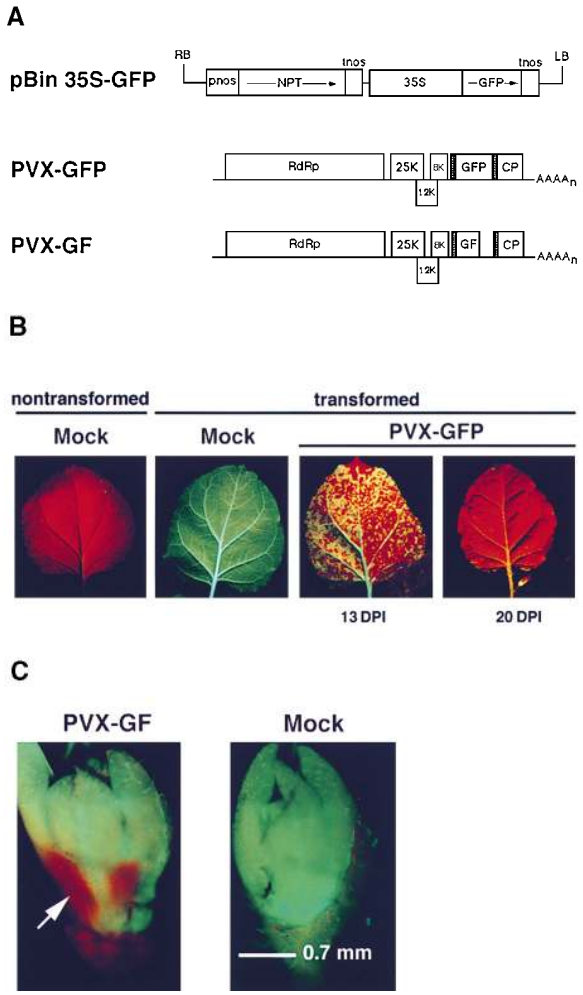

Figure 4. VIGS of the GFP.

(A) The organization of T-DNA constructs pBin 35S-GFP used for production of GFP transgenic plants and of PVX vectors used in VIGS of the GFP transgene. In the T-DNA construct, the promoters are pnos (nopaline synthase) and 35S; the transcriptional terminator is tnos (nopaline synthase); the T-DNA right and left borders are RB and LB, respectively; and the coding sequences are of the GFP and the neomycin phosphotransferase (NPT)–selectable marker gene. The PVX open reading frames are shown as RdRp (RNA-dependent RNA polymerase), 25K (25K protein), 12K (12K protein), 8K (8K protein), and CP (coat protein), and the inserts were the GFP open reading frame either intact or with the 3′ region deleted. In these vector constructs, the viral sequences were coupled to the 35S promoter and the plasmid DNA was inoculated directly to plants (Baulcombe et al., 1995). $AAAA_n$ represents the 3′-terminal polyA of the viral genome.
(B) The uppermost systemic leaves of plants that were either mock inoculated or inoculated with PVX–GFP, as indicated. The leaves were photographed under UV light at 13 and 20 DPI.
(C) The growing point of GFP transgenic plants photographed under UV light at 20 DPI with a mock inoculum or with PVX–GF. The arrow indicates the regions closest to the apical meristem in which VIGS of the GFP could be observed.

the loss of the green fluorescence (Figure 4B, 13 DPI). By 20 DPI, the youngest upper leaves were homogeneously red under UV illumination (Figure 4B, 20 DPI), indicating silencing of both intGFP and vGFP. PVX–GFP and PVX–GF both silenced intGFP to the same extent and over the same time course. IntGFP silencing was evident in roots, stems, seed capsules, and flowers and was most pronounced in the upper leaves and axillary shoots. In contrast, as shown in Figure 4C, the floral (data not shown) and vegetative apexes remained green fluorescent, indicating either that the virus had not entered these tissues or that they lacked the potential to silence GFP. In the third phase, beginning at ~28 DPI, VIGS of the GFP was maintained in parts of the plant that had already become silenced. However, there was faint green GFP fluorescence in the tissue emerging from the growing point, and by 41 DPI, the newly emerging tissue exhibited full GFP fluorescence.

GFP RNA Levels in Infected Plants

To assay the intGFP mRNA levels independently of the PVX–GFP RNA, we infected the transgenic *N. benthamiana* plants with PVX–GF and used the deleted 3′ part of the GFP sequence as probe in RNA gel blot analysis. The results are shown in Figure 5A. In the uppermost leaves of the plant at 13 DPI, the level of intGFP mRNA in the systemic leaves was below the limit of detection and at least 98% lower than in mock-inoculated plants. This decreased level of GFP mRNA corresponded to the second phase of VIGS in which there is a decrease in GFP (Figure 4). The uppermost leaves also contained low levels of intGFP mRNA at 20 DPI, but at 27 and 34 DPI, corresponding to the third phase of VIGS, the intGFP mRNA in these uppermost leaves was present at detectable levels (Figure 5A).

The level of PVX–GF RNA, detected with a GFP probe, also declined during the second phase of VIGS. However, the reduction in viral RNA, as shown in Figures 5B and 5C, was slower than the reduction of the intGFP mRNA. At 13 DPI, when intGFP mRNA was undetectable (Figure 5A), PVX–GF RNA was as abundant in the GFP transgenic plants as it was in the nontransgenic plants (Figures 5B and 5C). However, by 20 DPI, the PVX–GF in the GFP transgenic line was 95% lower than in nontransgenic plants (Figure 5B). The level further decreased and remained below the level of detection until 41 DPI, when the experiment was terminated (Figure 5C). The elimination of viral RNA corresponded to the third phase of GFP VIGS, as described above, when newly emerging leaves had progressively higher levels of GFP mRNA (Figure 5A). The levels of viral RNA exhibited similar kinetics when the GFP transgenic plants were inoculated with PVX–GFP (data not shown). These experiments indicate that VIGS of the GFP, unlike the PDS VIGS, is targeted against viral RNA as well as mRNA.

The analysis shown in Figure 5 was based on samples taken from the uppermost leaves in which VIGS would have

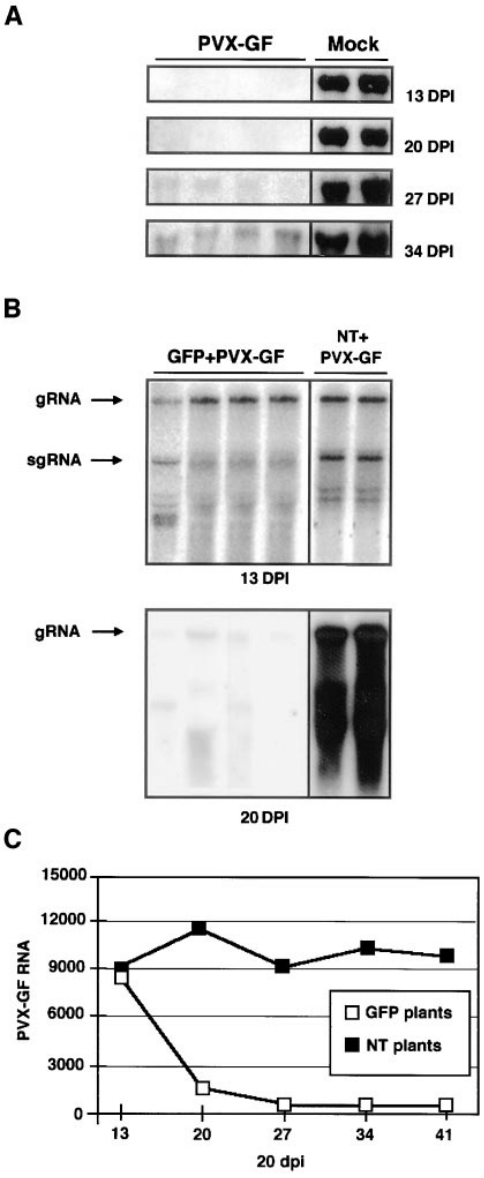

Figure 5. GFP RNA Levels.

(A) intGFP mRNA levels in mock-inoculated or PVX–GF—inoculated plants of *N. benthamiana* line GFP8. RNA samples were harvested at the indicated days postinoculation from the uppermost systemic leaves of plants, and 10 μg was loaded in each lane. Samples were assayed by RNA gel blotting, using a ^{32}P-labeled GFP cDNA as probe. Each lane corresponds to an individual plant.

(B) vGFP RNA in systemically infected leaves. RNA samples were taken at 13 and 20 DPI from the uppermost systemic leaves of GFP8 (GFP) or nontransgenic (NT) lines inoculated with PVX–GF. Equal amounts (10 μg) of each RNA sample were fractionated by agarose gel electrophoresis, and a ^{32}P-labeled RNA probe for PVX was used to detect the viral RNAs. The genomic (gRNA) and major subgenomic (sgRNA) RNA species are labeled. Each sample was analyzed in replicate, and the gel at the bottom was exposed longer than was the gel at the top to allow detection of the residual low levels of PVX–GF RNA in the samples from the GFP transgenic plants.

(C) vGFP RNA in systemically infected leaves. RNA samples were taken at the indicated DPI from the uppermost systemic leaves of GFP8 (GFP) or nontransgenic (NT) lines inoculated with PVX–GF. Equal amounts (10 μg) of each RNA sample were fractionated by agarose gel electrophoresis, and a ^{32}P-labeled RNA probe for PVX was used to detect the viral RNAs. The level of vGFP gRNA in each sample was quantified in terms of photostimulated luminescence units, using a PhosphorImager (see Methods). Each point represents the average value from three RNA samples.

been initiated recently. To investigate the maintenance of VIGS, we also analyzed GFP-silenced leaves lower down the plant at 21 DPI with PVX–GF or PVX–GFP. To determine whether there was persistence of VIGS targeted against viral RNA, these leaves were treated with a secondary inoculum of TMV carrying GFP (TMV–GFP). The genome organization of TMV–GFP is shown in Figure 6A, and the gel blot analysis of vGFP RNA accumulation was performed on samples taken 8 days after secondary inoculation (Figure 6B). There were abundant TMV–GFP RNAs and infection foci in leaves of nontransgenic plants that had been inoculated previously with PVX–GF or in the leaves of mock-inoculated transgenic plants (Figure 6B). In contrast, when the TMV–GFP inoculum was applied to the systemic, GFP-silenced leaves after 21 days, there were no GFP foci and the TMV–GFP RNA failed to accumulate (Figure 6B).

These data therefore confirm the persistence of VIGS targeted against viral RNAs. The gel blot data also show that the levels of PVX–GF RNA and intGFP mRNA were below the limits of detection in the lower leaves of plants exhibiting VIGS of GFP. The levels of vGFP RNA were further investigated by passage inoculation of sap extracts from the lower leaves of PVX–GFP—inoculated plants exhibiting VIGS of GFP. When inoculated to nontransformed plants, these extracts failed to produce green fluorescent infection foci, as would be expected if there had been accumulation of PVX–GFP. Also reflecting the absence of PVX–GFP or derivatives, these extracts failed to induce silencing of GFP when inoculated to GFP transgenic *N. benthamiana*. Therefore, from these combined back-inoculation data and the gel blot analysis (Figure 6), we conclude that VIGS persists, even in the absence of the inducing virus.

DISCUSSION

Separate Stages of VIGS

A key point from our analysis is the separation of initiation and maintenance stages of VIGS. Initiation of VIGS is absolutely

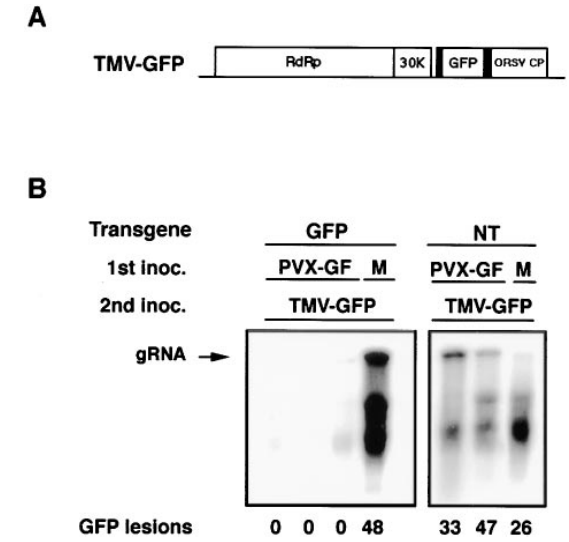

Figure 6. Virus Resistance Associated with VIGS of GFP.

(A) A TMV–GFP vector was used to analyze virus resistance in tissues exhibiting VIGS of the GFP transgene. The TMV open reading frames are shown as RdRp (RNA-dependent RNA polymerase), 30K (30K protein), and odontoglossum ringspot virus (ORSV) coat protein (CP) (Donson et al., 1991). The GFP open reading frame was inserted intact between duplicate CP promoters from the TMV and ORSV genomes (shaded boxes). The vector constructs were assembled as cDNA and transcribed into RNA for inoculation of plants.

(B) GFP8 (GFP) or nontransformed (NT) plants were inoculated initially (1st inoc.) with PVX–GF or were mock inoculated (M). After 21 DPI, the uppermost systemic leaves of these plants were given a second inoculum (2nd inoc.) of TMV–GFP; after another 8 days, the GFP infection foci were counted under UV light (GFP lesions). RNA samples (10 μg per lane) were analyzed by gel blotting, using a ^{32}P-labeled probe for GFP. The major genomic (gRNA) of TMV–GFP is indicated.

dependent on the virus. The target genes were not silenced unless the plants were infected with the corresponding viruses, and if the virus levels declined, VIGS was not initiated in the newly developing tissue at the growing point of the plant (Figure 5A). However, once initiated, VIGS of GFP persisted even in the absence of the inducing virus, indicating that the virus is not required for maintenance of VIGS. In the work described here, this virus-independent maintenance of VIGS was manifest as the continued absence of GFP (Figure 5) and the resistance against TMV–GFP (Figure 6) in the leaves from which the PVX–GF(P) had been eliminated.

In previous work with plants carrying viral cDNA transgenes, it has been shown that the "recovery" phenomenon is also a manifestation of virus-independent maintenance of VIGS. Recovery occurred in the upper parts of virus-infected plants, provided that there was a high degree of sequence similarity between the virus and the transgene (Lindbo et al., 1993; Tenllado et al., 1995). As occurred in the tissue exhibiting VIGS of the GFP (Figure 6), the recovered tissue was virus free but nevertheless showed continued silencing of the viral transgene and remained resistant against subsequent infection by the virus. It is likely that these distinct initiation and maintenance stages can explain the three phases of GFP VIGS. In the first phase of GFP VIGS, the plants exhibited vGFP fluorescence superimposed on the fluorescence from the intGFP. We envisage that during this first phase of VIGS, there would be virus-dependent initiation of VIGS in all of the PVX–GF(P)—infected tissue but that the silencing phenotype would not yet be evident. In the second phase of GFP VIGS, there would be initiation and maintenance in different parts of the plant. Initiation would be taking place in infected cells at the base of the growing point of the plant, and consistent with this interpretation, we found that second-phase plants contain high levels of PVX–GF(P) in the apical zones (data not shown). At the same time, in the GFP-silenced regions of the plant, there would be maintenance of VIGS, resulting in progressive loss of vGFP and intGFP fluorescence from leaves and stems that previously had been infected with PVX–GF(P). In the third phase, the lower leaves of the plant would continue to exhibit maintenance of GFP VIGS. These leaves remained free of intGFP fluorescence and were resistant to inoculation with GFP virus. However, in the growing point, the progressive spread of VIGS through the plant would likely have caused complete elimination of PVX–GF(P). The absence of PVX–GF(P) would mean that VIGS would not be induced in the newly developing leaves and consequently would explain the late increase that we observed in the levels of intGFP RNA and fluorescence. This third phase of VIGS has not been described previously in plants carrying viral cDNA transgenes that were undergoing virus-induced "recovery" (Lindbo et al., 1993; Tenllado et al., 1995). We consider that this difference may be due to the transgene constructs or because the previous experiments were terminated before the third phase had begun.

Initiation of VIGS

Initiation of VIGS could be determined by an interaction of the viral RNA with the corresponding nuclear gene or at the RNA level with the mRNA. Alternatively, VIGS could be initiated by the virus, independently of the nuclear gene. Neither hypothesis can be ruled out definitively. However, our data are more easily reconciled with the nuclear gene–independent hypothesis because the initiation of VIGS against PDS and GFP was similar. If the nuclear genes were involved, it would be expected that initiation of PDS VIGS would be slower or less efficient than GFP VIGS because PDS and GFP are such different genes: PDS is an endogenous gene expressed at a low level, whereas GFP is a transgene ex-

pressed at a high level. Furthermore, also consistent with a nuclear gene–independent role of the virus in VIGS, we have shown elsewhere that viruses without similarity to a nuclear gene can initiate a gene silencing–like mechanism (Ratcliff et al., 1997). For these various reasons, we favor the explanation that viral RNA initiates VIGS independently of the corresponding nuclear gene or mRNA.

The proposed independent role of the virus as an initiator of VIGS, independent of the nuclear gene, could be accommodated in a model of transgene silencing based on work performed on petunia and might point to a similarity of these two categories of gene silencing. The model invoked RNA double strandedness as an initiator of gene silencing (Metzlaff et al., 1997). In the petunia model, the double strandedness was due to secondary structures in the silenced mRNA; in virus-infected cells, the double-stranded RNA exists, at least transiently, as a viral replication intermediate (Matthews, 1991). A role for double-stranded RNA in gene silencing could also explain the recent finding (Angell and Baulcombe, 1997) that transgenes encoding replicating viral RNAs are efficient activators of post-transcriptional gene silencing. Our finding that initiation of PDS VIGS is independent of the orientation of the insert (Figure 2) is also consistent with this proposed involvement of double-stranded RNA.

Maintenance of VIGS

Although a case can be made that initiation of VIGS is independent of the corresponding nuclear gene, the maintenance stage of VIGS is clearly influenced by the nuclear gene. This influence is indicated by the differential effects of VIGS on PVX–PDS and PVX–GFP. There was no suppression of PVX–PDS associated with VIGS of PDS, whereas there was suppression of PVX–GFP during the maintenance of VIGS against the GFP. Our interpretation of this difference is that after the initiation of VIGS of GFP, the GFP transgene produces a factor that has two interrelated activities. One of these activities leads to suppression of PVX–GF(P), whereas the second activity is responsible for maintenance of VIGS in cells from which the PVX–GF(P) has been eliminated. To account for the sequence specificity of VIGS, we propose that this factor has GFP RNA as a component.

Why is PVX–PDS not a target of VIGS? Based on findings that the 3′ end of transgene mRNAs is the target of gene silencing, one explanation could be that the PDS constructs all lack the 3′ end of the PDS mRNA (English et al., 1996; Sijen et al., 1996). However, we do not favor that explanation because there are other analyses, including the VIGS of the GFP described here, showing that targets of gene silencing may be other than at the 3′ end of the target gene (Marano and Baulcombe, 1998). We consider it more likely that the PDS endogenous gene does not produce the hypothetical RNA-containing factor that was invoked above to account for VIGS of the GFP. Alternatively, it could be that the PDS VIGS factor is too rare or lacks an essential feature required for targeting of viral RNA. In this situation, because the hypothetical factor also is required for maintenance of VIGS, the mechanism underlying PDS VIGS would not progress beyond the initiation stage. However, PDS VIGS would persist in the plant because of the continued presence of the PVX–PDS. Alternatively, it could be that the RNA-containing factor is produced in the PVX–PDS—infected cell and that it is able to maintain VIGS of PDS but unable to target PVX–PDS effectively. In this instance, the continuing high level of PVX–PDS would have masked the involvement of the factor in persistent VIGS of PDS.

A Role for VIGS and Possible Applications

From the proposed nuclear gene–independent initiation of VIGS, it is predicted that gene silencing would be initiated in cells infected with wild-type PVX as well as with the PVX vector constructs described here. The wild-type virus would accumulate and activate gene silencing that would be targeted against its own RNA. As a result of PVX-targeted gene silencing, PVX replication would slow down. However, in the absence of a homologous nuclear transgene, there would be no RNA-containing factors produced to maintain the gene-silencing mechanism. The suggestion that wild-type viruses elicit gene silencing also has been made by others and is based on the finding that accumulation of PVX and other viruses is higher in cells that are also infected with a potyvirus than in singly infected cells (Pruss et al., 1997). A model was developed in which VIGS is a mechanism that normally restricts virus accumulation in the infected cell and thereby increases accumulation of the other virus in cells that are infected with a potyvirus and a second type of virus (Pruss et al., 1997). The phenomena in which wild-type viruses initiate a gene silencing–like resistance mechanism (Covey et al., 1997; Ratcliff et al., 1997) are also consistent with that hypothesis.

There are several potential applications of VIGS. The simplest is as a tool in reverse genetics analysis of gene function. It would be possible to silence a gene by VIGS and thereby determine the role of the gene product much more quickly than by using antisense or sense suppression. This approach would be particularly suited to essential genes that would have lethal phenotypes in mutant or transgenic plants. It also will be possible to use cDNA libraries in a forward genetics approach based on VIGS. From the patterns of VIGS that we have observed here, it seems likely that genes expressed in many tissues could be silenced by VIGS. However, genes expressed in meristems may not be affected either because viruses do not generally penetrate meristematic zones (Matthews, 1991) or because the mechanisms of gene silencing do not operate in meristems (Tanzer et al., 1997).

METHODS

Green Fluorescent Protein–Transformed Lines

Four independent green fluorescent protein (GFP) lines (GPF8, GFP16c, GFP17b, and GFPY) of *Nicotiana benthamiana* plants carrying the mGFP5 transgene (Haseloff et al., 1997) were generated by the *Agrobacterium tumefaciens* leaf disc transformation method (Horsch et al., 1985). For transformation, the disarmed Agrobacterium strain GV-3101 containing the binary vector pBin-35S-mGFP5 (Haseloff et al., 1997) was used. DNA gel blot analysis performed as described by Mueller et al. (1995) showed that each line harbored a single T-DNA integration site, which is consistent with the observed 3:1 segregation of GFP expression in the R_1 generation. In all cases, this single locus was associated with one intact copy of the transgene. The four lines exhibited comparable high levels of GFP mRNA, as determined by RNA gel blot analysis. The plants used in this work were homozygous, selfed F_1 progeny of the primary transformants. The data presented here were obtained with line GFP8 unless otherwise stated, but identical results were generated using the other three GFP lines.

Construction of Potato Virus X (PVX) Derivatives, in Vitro Transcription, and PVX Infection

Cloned copies of wild-type PVX (pTXS) (Kavanagh et al., 1992) as well as the PVX vectors pP2C2S and pPVX–GFP (Baulcombe et al., 1995) have been described previously. PVX–GF was made by replacing the original GFP insert in pPVX204 (Baulcombe et al., 1995) with the mGFP5 insert from pBin-35S-mGFP5 (Haseloff et al., 1997) and by removing the 354-bp fragment between a ClaI site (position 465 within the GFP5 coding sequence) and a SalI site at the 3′ end of GFP5 (position 818). PVX–PDS and PVX–SDP, PVX–PDS^{def} and PVX–SDP^{def}, and PVX–5′PDS and PVX–5′SDP were generated by cloning into the PVX vector pP2C2S the corresponding reverse polymerase chain reaction (PCR) product in the sense or antisense orientation, respectively. The PCR products had been obtained using primers homologous to regions of the tomato PDS cDNA (Pecker et al., 1992) exhibiting high homology with other Solanaceae species (positions 445 to 468 [upstream] and 803 to 825 [downstream] for insert in PVX–5′PDS and PVX–5′SDP; 1300 to 1321 [upstream] and 1692 to 1712 [downstream] for insert in PVX–PDS and PVX–SDP; and 1499 to 1521 [upstream] and 1692 to 1712 [downstream] for insert in PVX–PDS^{def} and PVX–SDP^{def}). PVX–INT and PVX–TNI were made by cloning into pP2C2S a PCR product from an intron present in the part of the *N. benthamiana* PDS gene spanned by the cDNA fragment present in PVX–PDS^{def}. The positions of the primers used to generate the PCR fragment present in PVX–INT and PVX–TNI were 24 to 46 (upstream) and 223 to 248 (downstream) of the *N. benthamiana* intron corresponding to intron 10 in the tomato gene. The fragment present in the PVX–5′UTR and PVX–5′RTU constructs was a product of inverse PCRs (Brigneti et al., 1997) performed on *N. benthamiana* genomic DNA treated with RsaI (primers extending from positions −173 to −151 [upstream] and −6 to −28 [downstream] from the *N. benthamiana* initiation codon). All of the constructs were verified by double-stranded sequencing using PRISM dye terminator cycle sequencing, according to the directions of the manufacturer (Applied Biosystems, Foster City, CA).

In vitro transcription reactions to produce infectious PVX RNA were performed as described previously (Chapman et al., 1992). For the study of PDS silencing, infectious RNA was rubbed onto the leaves of 4- to 5-week-old wild-type *N. benthamiana* plants in the presence of a small amount of carborundum. For GFP silencing, plasmid DNA containing the corresponding viral constructs under the control of the 35S promoter were directly inoculated onto *N. clevelandii* (Baulcombe et al., 1995). Virus bulked up from these infected plants was then used to inoculate GFP transgenic plants of the same age.

Reverse Transcription–PCR

Total RNA from plant tissue was obtained as previously described (Mueller et al., 1995), treated with RNase-free DNase (Promega), and recovered by ethanol precipitation. Normally, 1 μg of total RNA was mixed with 500 ng of oligo(dT)$_{12–18}$ primer (Pharmacia) in a total volume of 13.5 μL, heated at 65°C for 5 min, and cooled in ice. Reverse transcription (RT) was performed in a total volume of 40 μL containing the RNA and primer mixture; 1 × RT buffer (Gibco BRL); 1.25 mM dATP, dCTP, dGTP, and dTTP; 10 mM DTT; 1 unit of RNase inhibitor (Pharmacia); and 400 units of Superscript reverse transcriptase (Gibco BRL) for 1 hr at 37°C and then heated at 95°C for 1 min. The PCR reactions were performed in a total volume of 50 μL consisting of 2 μL of the RT reaction; 1 × PCR buffer (Rommens et al., 1995); 200 μM dATP, dCTP, dGTP, and dTTP; 40 nM each of sense and antisense primers; and 5 units of Taq DNA polymerase. Control reactions without reverse transcriptase were routinely used to assess the presence of any contaminating DNA.

For RNA abundance assay, aliquots of the DNase-treated samples, containing between 5 and 500 ng of total RNA, were used in the RT reactions. Aliquots (2 μL) of these samples provided the template in separated PCR reactions performed using primers specific for either PDS (at coordinates 1300 to 1321 [upstream] and 2093 to 2115 [downstream] to specifically amplify the endogenous PDS and not those fragments present in the PVX constructs) or ubiquitin (their sequence corresponding to highly conserved regions in ubiquitin from different Solanaceae species: positions 48 to 68 [upstream] and 240 to 260 [downstream] of the *N. sylvestris* ubiquitin polygene 11 [Genschik et al., 1992]). The PCR reactions were performed for 30 cycles (15 sec at 94°C, 15 sec at 55°C, and 30 sec at 72°C), with a final extension at 72°C for 10 min. Ten microliters of the total reaction volumes was used for electrophoresis on 1% agarose gels in Tris–borate–EDTA buffer. The DNA was transferred with denaturing solution (1.5 M NaCl, 0.5 M NaOH) onto nylon membranes and hybridized with the corresponding ^{32}P-labeled probes. The PDS probe was the cDNA (sequence positions 1300 to 1712) present in the PVX–PDS construct. The ubiquitin probe was a 1.8-kb EcoRI fragment of pSAM293, which is a cDNA clone from *Antirrhinum majus* (GenBank accession number X67957). The signals obtained were quantified using Fujix Bio-Imaging Analyzer Bas 1000 (Fuji Photo Film Co., Ltd., Fuji, Japan) equipment. PDS mRNA content was expressed as photostimulated luminescence units per nanogram of total RNA, as calculated from the ubiquitin signal.

RNA Gel Blot Analysis

RNA gel blot analysis was performed as described previously (Mueller et al., 1995). A ^{32}P-labeled RNA probe corresponding to the 3′-terminal 1562 bases of PVX was used to determine total viral content. The DNA fragments used as probes were labeled by random

priming incorporation of ^{32}P-dCTP. A 409-bp PDS cDNA fragment corresponding to the segment present in the PVX–PDS and PVX–SDP constructs was used as a specific probe for recombinant viruses. The whole GFP cDNA was used to detect both viral GFP (vGFP) and integrated GFP (intGFP) mRNA, whereas the 354-bp 3′-terminal fragment of intGFP cDNA, which was named P, was used to differentiate intGFP mRNA and viral RNA from plants infected with PVX–GF. After hybridization, the signal present in the membranes was analyzed and quantified using the equipment described above.

ACKNOWLEDGMENTS

We are grateful to the Gatsby Charitable Foundation for support of this work, to Andrew Hamilton and Vicki Bowman Vance for valuable discussion, and to Guy F. Davenport for the TMV–GFP construct.

Received February 9, 1998; accepted April 13, 1998.

REFERENCES

Angell, S.M., and Baulcombe, D.C. (1997). Consistent gene silencing in transgenic plants expressing a replicating potato virus X RNA. EMBO J. **16,** 3675–3684.

Baulcombe, D.C. (1996a). Mechanisms of pathogen-derived resistance to viruses in transgenic plants. Plant Cell **8,** 1833–1844.

Baulcombe, D.C. (1996b). RNA as a target and an initiator of post-transcriptional gene silencing in transgenic plants. Plant Mol. Biol. **32,** 79–88.

Baulcombe, D.C., Chapman, S.N., and Santa Cruz, S. (1995). Jellyfish green fluorescent protein as a reporter for virus infections. Plant J. **7,** 1045–1053.

Brigneti, G., Garcia-Mas, J., and Baulcombe, D.C. (1997). Molecular mapping of the potato virus Y resistance gene (*Ry$_{sto}$*) in potato. Theor. Appl. Genet. **94,** 198–203.

Chalfie, M., Tu, Y., Euskirchen, G., Ward, W.W., and Prasher, D.C. (1994). Green fluorescent protein as a marker for gene expression. Science **263,** 802–805.

Chapman, S.N., Kavanagh, T.A., and Baulcombe, D.C. (1992). Potato virus X as a vector for gene expression in plants. Plant J. **2,** 549–557.

Covey, S.N., Al-Kaff, N.S., Langara, A., and Turner, D.S. (1997). Plants combat infection by gene silencing. Nature **385,** 781–782.

Demmig-Adams, B., and Adams, W.W. (1992). Photoprotection and other responses of plants to high light stress. Annu. Rev. Plant Physiol. Plant Mol. Biol. **43,** 599–626.

Depicker, A., and Van Montagu, M. (1997). Post-transcriptional gene silencing in plants. Curr. Opin. Cell Biol. **9,** 372–382.

Donson, J., Kearney, C.M., Hilf, M.E., and Dawson, W.O. (1991). Systemic expression of a bacterial gene by a tobacco mosaic virus–based vector. Proc. Natl. Acad. Sci. USA **88,** 7204–7208.

English, J.J., Mueller, E., and Baulcombe, D.C. (1996). Suppression of virus accumulation in transgenic plants exhibiting silencing of nuclear genes. Plant Cell **8,** 179–188.

Genschik, P., Parmentier, Y., Durr, A., Marbach, J., Criqui, M.C., Jamet, E., and Fleck, J. (1992). Ubiquitin genes are differentially regulated in protoplast-derived culture of *Nicotiana sylvestris* and in response to various stresses. Plant Mol. Biol. **20,** 897–910.

Giuliano, G., Bartley, G.E., and Scolnik, P.A. (1993). Regulation of carotenoid biosynthesis during tomato development. Plant Cell **5,** 379–387.

Goodwin, J., Chapman, K., Swaney, S., Parks, T.D., Wernsman, E.A., and Dougherty, W.G. (1996). Genetic and biochemical dissection of transgenic RNA-mediated virus resistance. Plant Cell **8,** 95–105.

Guo, H.S., and Garcia, J.A. (1997). Delayed resistance to plum pox potyvirus mediated by a mutated RNA replicase gene: Involvement of a gene-silencing mechanism. Mol. Plant-Microbe Interact. **10,** 160–170.

Haseloff, J., Siemering, K.R., Prasher, D.C., and Hodge, S. (1997). Removal of a cryptic intron and subcellular localization of green fluorescent protein are required to mark transgenic *Arabidopsis* plants brightly. Proc. Natl. Acad. Sci. USA **94,** 2122–2127.

Horsch, R.B., Fry, J.E., Hoffmann, N.L., Eichholtz, D., Rogers, S.G., and Fraley, R.T. (1985). A simple and general method of transferring genes into plants. Science **227,** 1229–1231.

Kavanagh, T.A., Goulden, M., Santa Cruz, S., Chapman, S.N., Barker, I., and Baulcombe, D.C. (1992). Molecular analysis of a resistance-breaking strain of potato virus X. Virology **189,** 609–617.

Kumagai, M.H., Donson, J., Della-Cioppa, G., Harvey, D., Hanley, K., and Grill, L.K. (1995). Cytoplasmic inhibition of carotenoid biosynthesis with virus-derived RNA. Proc. Natl. Acad. Sci. USA **92,** 1679–1683.

Lindbo, J.A., Silva-Rosales, L., Proebsting, W.M., and Dougherty, W.G. (1993). Induction of a highly specific antiviral state in transgenic plants: Implications for regulation of gene expression and virus resistance. Plant Cell **5,** 1749–1759.

Mann, V., Pecker, I., and Hirschberg, J. (1994). Cloning and characterization of the gene for phytoene desaturase from tomato (*Lycopersicon esculentum*). Plant Mol. Biol. **24,** 429–434.

Marano, M.R., and Baulcombe, D. (1998). Pathogen-drived resistance targeted against the negative-strand RNA of tobacco mosaic virus: RNA strand-specific gene silencing? Plant J. **13,** 537–546.

Matthews, R.E.F. (1991). Plant Virology, 3rd ed. (San Diego, CA: Academic Press).

Metzlaff, M., O'Dell, M., Cluster, P.D., and Flavell, R.B. (1997). RNA-mediated RNA degradation and chalcone synthase A silencing in petunia. Cell **88,** 845–854.

Mueller, E., Gilbert, J.E., Davenport, G., Brigneti, G., and Baulcombe, D.C. (1995). Homology-dependent resistance: Transgenic virus resistance in plants related to homology-dependent gene silencing. Plant J. **7,** 1001–1013.

Pecker, I., Chamovitz, D., Linden, H., Sandmann, G., and Hirshren, J. (1992). A single polypeptide catalyzing the conversion of phytoene to *z*-carotene is transcriptionally regulated during tomato fruit ripening. Proc. Natl. Acad. Sci. USA **89,** 4962–4966.

Pruss, G., Ge, X., Shi, X.M., Carrington, J.C., and Bowman Vance, V. (1997). Plant viral synergism: The potyviral genome encodes a broad-range pathogenicity enhancer that transactivates replication of heterologous viruses. Plant Cell **9,** 859–868.

Ratcliff, F., Harrison, B.D., and Baulcombe, D.C. (1997). A similarity between viral defense and gene silencing in plants. Science **276,** 1558–1560.

Rommens, C.M.T., Salmeron, J.M., Oldroyd, G.E.D., and Staskawicz, B.J. (1995). Intergeneric transfer and functional expression of the tomato disease resistance gene *Pto*. Plant Cell **7,** 1537–1544.

Sijen, T., Wellink, J., Hiriart, J.-B., and Van Kammen, A. (1996). RNA-mediated virus resistance: Role of repeated transgenes and delineation of targeted regions. Plant Cell **8,** 2277–2294.

Smith, H.A., Swaney, S.L., Parks, T.D., Wernsman, E.A., and Dougherty, W.G. (1994). Transgenic plant virus resistance mediated by untranslatable sense RNAs: Expression, regulation, and fate of nonessential RNAs. Plant Cell **6,** 1441–1453.

Tanzer, M.M., Thompson, W.F., Law, M.D., Wernsman, E.A., and Uknes, S. (1997). Characterization of post-transcriptionally suppressed transgene expression that confers resistance to tobacco etch virus infection in tobacco. Plant Cell **9,** 1411–1423.

Tenllado, F., Garcia-Luque, I., Serra, M.T., and Diaz-Ruiz, J.R. (1995). *Nicotiana benthamiana* plants transformed with the 54-kDa region of the pepper mild mottle tobamovirus replicase gene exhibit two types of resistance response against viral infection. Virology **211,** 170–183.